Facies characteristics of aeolianites near Atlit - Carmel coastal plain, Israel

by

ALEXANDER NEBER, WOLFGANG BOENIGK, AVRAHAM RONEN

With 4 Figures

Addresses of the authors:
ALEXANDER NEBER, WOLFGANG BOENIGK
Geologisches Institut, Abteilung Quartärgeologie
Universität zu Köln
Zülpicher Str. 49a
50674 Köln
Germany
Fax: **49-(0)221-470-5149
E-mail: a.neber@uni-koeln.de

AVRAHAM RONEN
Zinman Institute of Archaeology
University of Haifa
Haifa 31905
Israel

Contents

Abstract

The morphology of the Mediterranean coastal plain of Israel is dominated by coast parallel dune ridges of Quaternary age. This study focuses on an exposed succesion at the "Atlit Railroad Bridge" in the Carmel coastal plain, which is comprised of four carbonated aeolianites ("kurkar"), inter-bedded paleosols (mostly "hamra"), and one beachrock horizon. The aeolianites are characterized by variations in lithology and petrography due to facies differences during deposition and early diagenesis. In general, the aeolianites formed under semi-arid conditions, whereas soils developed during humid periods. Initial sand encroachment is documented by transverse ridges of barchanoid like dunes. Further sand accumulation resulted in a vertical growth of the dune sequence, when sand migration was hampered by a vegetation cover. The temporal succession of the aeolianites is given by luminescence age estimates from late OIS 6 onward. The associated climate record is in phase with environmental fluctuations from continental and marine climate archives in the eastern Mediterranean and northern Africa.

1. Introduction

The Mediterranean coastal plain of Israel is characterized by coastal dune ridges of Quaternary age. These elongated ridges run parallel to the current shoreline and are generally comprised of carbonated aeolianites (locally termed "kurkar") and interbedded paleosols (locally termed "hamra"). The investigated sites between Haifa and Atlit also incorporate a distinct beachrock horizon. The coastal dunes of the Central coastal plain, extending from Haifa to Tel Aviv (Fig. 1), formed during blow out processes along the beaches. The beaches themselves are nourished by clastic sediments from the Nile delta brought through Mediterranean counterclockwise longshore currents along the coasts of Sinai and Israel (Emery & Neev 1960, Goldsmith & Golik 1980).

The sedimentological, petrographical, and genetical relationships of the aeolian sediments and paleosols, the associated changes in environment and climate, as well as the stratigraphical position and temporal succession of the
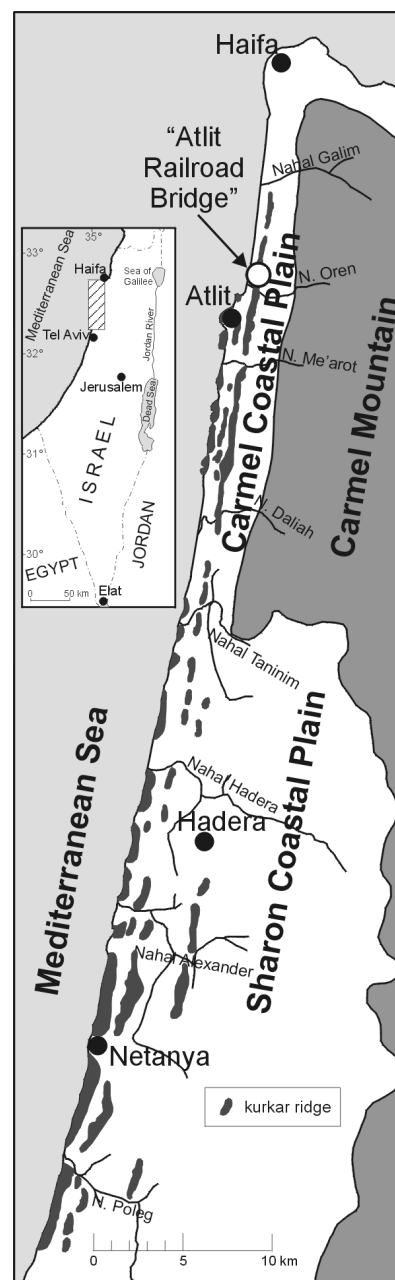

Fig. 1: Map showing distribution of kurkar ridges in the Central coastal plain and the location of study area.

deposits have been widely discussed in literature in the past decades. AVNIMELECH (1962) and ISSAR (1968, 1980) proposed that each of the "kurkar ridges" represents a single accumulation phase, that the age of the sandstone ridges decreases from east to west, and that each ridge is related to a respective fossil shoreline. Soil forming periods have been generally related to regressive marine stages and episodes of enhanced precipitation (e.g. YAALON & DAN 1967, ISSAR & PICARD 1971). Studies of KARMELI et al. (1968), FARRAND & RONEN (1974), RONEN (1975), GVIRTZMAN et al. (1984), and BOENIGK et al. (1985) document that the coastal dune ridges are the result of several multi-phase and complex cyclical events of sand accumulation and soil development. NEEV et al. (1987) proposed several phases of tectonic activity along coast parallel lineaments during the Quaternary, which caused the linear morphological extension of the "kurkar ridges". GVIRTZMAN et al. (1998) concluded that the shore near "kurkar ridges" in the Sharon coastal plain are typical longitudinal dunes, which result from coast parallel winds, and formed simultaneously during the Last Glacial Stage. TSOAR (2000) rejected this proposed model of longitudinal dunes for the "kurkar ridge" formation and suggested that the elongated ridges formed from typical foredunes.

A relative stratigraphy of the deposits is given by archaeological implement bearing horizons. Archaeological finds in the Carmel coastal plain of Middle Paleolithic age are strictly confined to paleosols, demonstrating that the coastal plain was deserted by humans during periods of sand accumulation (FARRAND & RONEN 1974, RONEN 1975, 1977). Numerical radioluminescence age estimates for the Quaternary sequences in the Carmel coastal plain have been published by RONEN et al. (1999), showing major soil formation episodes in oxygen isotopic stage (OIS) 5 and OIS 4.

This study is part of a multidisciplinary project funded by the German-Israeli Foundation for Scientific Research and Development, combining sedimentology, pedology, archaeology, and geochronology. The aim of the project was to obtain a detailed and reliable chronological framework based on luminescence age estimates for the Quaternary sequences along the Central coastal plain of Israel, in order to estimate the duration of desertification episodes and periods of human habitation. The established luminescence ages of key sections along the Carmel coastal plain and a detailed chronostratigraphy are given in NEBER (2002). Methodological aspects of the dating procedures, as equivalent dose and palaeodose determination, bleaching experiments, etc., will be presented in a further publication by FRECHEN et al. (in prep.).

This article focuses on macro- and microscopic characteristics of the aeolianites, exposed near the "Atlit Railroad Bridge", in order to establish facies criteria, to verify depositional and early diagenetic textures as well as their relation to local or regional climate fluctuations during the Quaternary.

2. Methodology

The Quaternary sequence at the "Atlit Railroad Bridge" (Fig.1, Fig. 2) exposes several aeolianites, an intercalated beachrock horizon, and interbedded as well as a covering
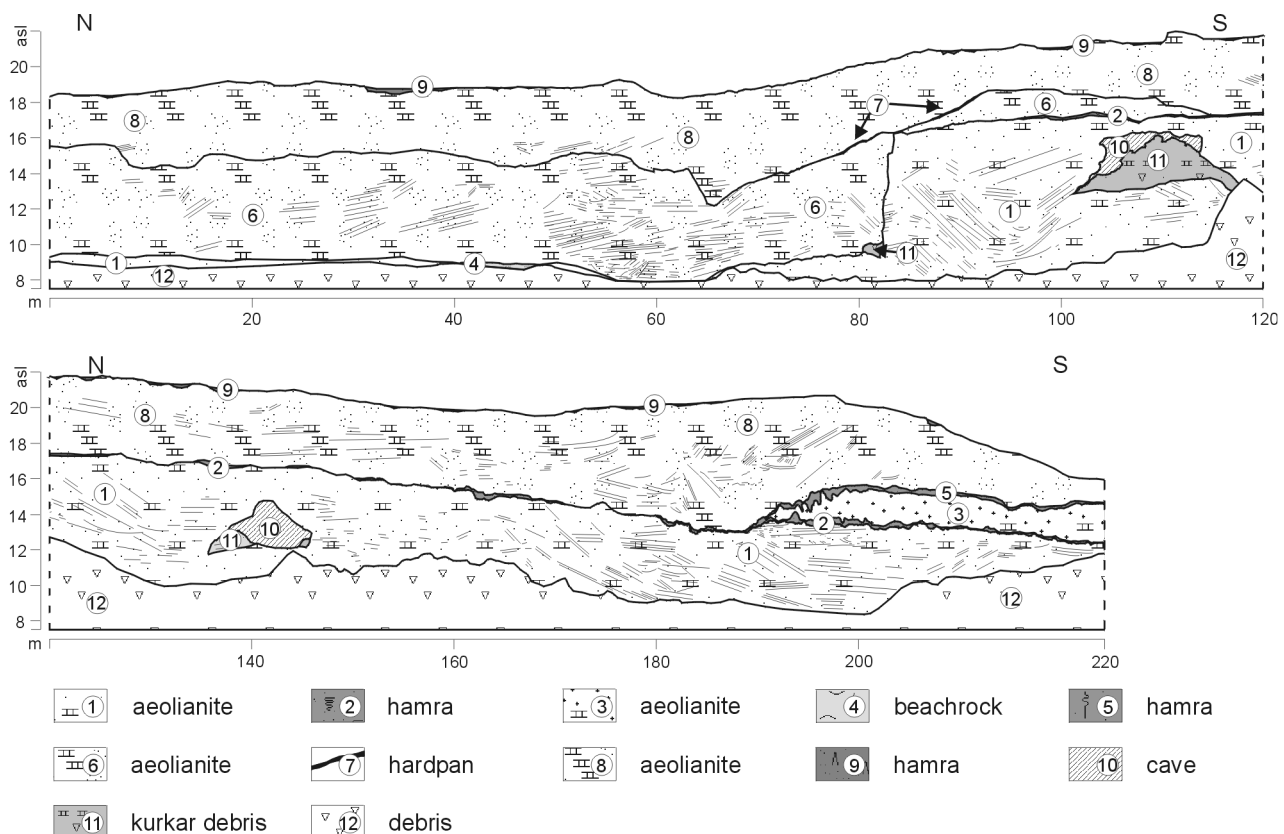

Fig. 2: Cross section of the "Atlit Railroad Bridge" site. Vertical exaggeration x 1,5.

paleosols. The particle size distribution was determined on dry samples after homogenization and removal of carbonates by hydrochloric acid. Sieve sizes were chosen according to the UDDEN-WENTWORTH φ grade scale for grain sizes with mash sizes of φ grades from 0 to 5. Median and mean grain sizes, sorting, skewness, and kurtosis (FOLK & WARD 1957) were calculated using SediVision 3.0 (Beguma GbR, Berlin, Germany). Early diagenetic lithification processes of the exposed aeolianites and beachrock were investigated in thin sections based on studies by FRIEDMAN (1964), GAVISH & FRIEDMAN (1969), and ADAMS & MACKENZIE (1998). Infrared spectra (IRS) were obtained by a Fourier Transform Infrared Spectrometer (Midac Corp., Mesa, California) using potassium bromide pellets at 4 cm^{-1} collection resolution. A HC2-LM hot cathode (NEUSER 1988, 1997) was used for cathodoluminescence (CL) analysis which have been performed at operating conditions of 14 keV beam energy, 15 μA mm^{-2} beam-current density, and 10^{-6} torr operating vacuum. Elemental distribution maps of Mg, Na, Sr, Fe, and Mn were obtained by means of electron microprobe analysis (EMPA) using a JXA-8900 RL microprobe (Jeol Ltd., Peabody, MA, USA) operating at 20 kV accelerating voltage and 40 nA beam-current density.

3. Results

3.1. Geological setting and temporal succession of the sediments

The outcrop at the "Atlit Railroad Bridge" (ARB) displays a complex geological history, documented by nine lithological units (Fig. 2). A conceptual sedimentological model is depicted in Figure 3 and the temporal succession of the deposits, given by luminescence ages in NEBER (2002) and from FRECHEN et al. (in prep.), is visualized in Figure 4.

The visible base of the ARB section is composed of an indurated aeolianite (Unit 1) which is characterized by its massive appearance, whitish color and preserved cross-bedding structures. The foresets are mostly tabular planar and dip predominantly in westerly directions. This kurkar is covered by a carbonated reddish, sandy hamra (Unit 2), which formed in situ. Unit 3 is a massive grayish, nodular aeolianite with carbonate concretions and abundant rhizolithes. This kurkar is only preserved in the southern part of the section. The basal aeolianite (Unit 1) is truncated by a vertical transition, resembling a "paleo-cliff". Along the suggested abrasion platform beachrock has been deposited (Unit 4) at an elevation of approximately 9 m above sea level. The kurkar B type aeolianite (Unit 3) in the southern fringe of the site is covered by a sandy and weakly cemented, reddish hamra (Unit 5). The morphological negative form of the "paleo-cliff" in the northern part of the section is filled with kurkar material (Unit 6). This grayish and partly nodular kurkar shows weakly preserved tabular planar beds of moderately high dipping angles to the northwest. Reduced sand accumulation after the deposition of Unit 6 is documented by a carbonaceous, caliche-like hardpan (Unit 7). The whole site is covered by a massive grayish, nodular aeolianite (Unit 8). This uppermost kurkar is characterized by abundant rhizolithes and weakly preserved bedding structures of tabular planar beds which show low angle dips to the northwest. Cavities on top of the Unit 8 kurkar are filled by brownish sandy loam hamra (Unit 9). Two caves (Unit 10) developed within the aeolian sandstone of Unit 1.
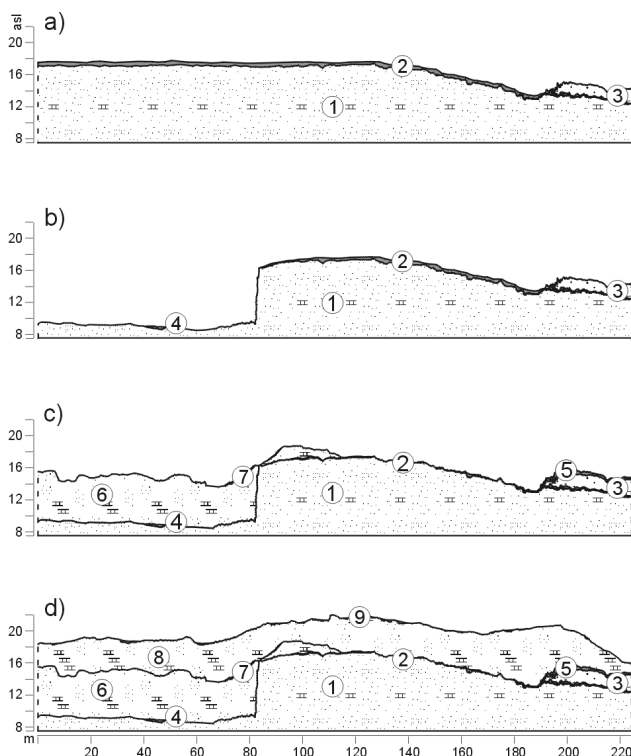
3.2. Particle size analysis of aeolianites and beachrock

The lowermost part of the Unit 1 aeolianite at the ARB section is well sorted with median and mean grain sizes around 2.53 φ, changing gradually into a moderately well sorted sediment with median and mean values of 2.56 φ in the uppermost part of the unit. All samples of Unit 1 show a positive skewness and a mesokurtic kurtosis. The kurkar of Unit 3 is characterized by a coarser grain size with median and mean grain sizes around 2.25 φ, as well as a negative skewness and mesokurtic kurtosis. In contrast, the exposed beachrock (Unit 4) is moderately well sorted, median and mean grain sizes are given with 2.62 to 2.73 φ, and the skewness is very positive and kurtosis very leptokurtic. Subsequent aeolian sedimentation is documented by the kurkars of Unit 6 and of Unit 8. The Unit 6 aeolianite is very well to well sorted, with median and mean grain sizes around 2.45 φ. Skewness is negative to nearly symmetrical and kurtosis mesokurtic. The uppermost aeolianite of Unit 8 is generally well to moderately

Fig. 3: Schematic sketch. Geological history of section "Atlit Railroad Bridge". a) Aeolianite deposition and subsequent hamra development, succeeded by aeolianite accumulation. b) Marine transgression and beachrock deposition. c) Hamra formation, aeolianite deposition and hardpan development. d) Aeolianite accumulation followed by hamra development. See Fig. 2 for legend.

well sorted with finer grained median and mean values around 2.50 φ as well as a nearly symmetrical to positive skewness and meso- to leptokurtic kurtosis.

In summary, the exposed beachrock and aeolianites show distinct particle size attributes, expressed by varying median and mean values as well as associated changes in skewness and kurtosis (Fig. 4).

3.3. Petrography and mineralogy of aeolianites

The main rock-forming mineral is subangular to subrounded quartz, accompanied by feldspar, accessory heavy minerals, and varying amounts of fossil components (Fig. 4). The fossil assemblage is usually represented by abraded marine shells and fragments of mollusks, coralline algae, red algae, echinoidea, and benthic foraminifera (mostly *Miliolidea*). The aeolianites show distinct characteristics in petrography which are related to alteration processes of minerals and carbonate cement precipitation. Quartz grains in thin sections from aeolianites of Unit 1, Unit 6, and Unit 8 show corroded grain margins. These corrosion embayments result from silica replacement by carbonate cements during early diagenesis. Rhizocretions are common in all aeolianites, but most abundant in the Unit 3 kurkar, and are documented by fine grained quartz fragments in a brown micritic matrix surrounding former roots. Rock-forming particles adjacent to rhizocretions show well developed brownish micritic rims of fibrous needle like fabric. The Unit 6 and Unit 8 aeolianites are characterized by ooids with up to three concentric layers,

superficial ooids, around quartz nuclei. Early diagenetic lithification in all studied aeolianites is documented by several distinct generations of pore-occluding cements. In general, the interparticle space has been occluded by isopachous cement, grown perpendicularly to the surface of particles. These micritic cements are succeeded by micro-sparitic to sparitic carbonate, resembling a drusy mosaic. The latter cements are more pronounced in the aeolianites of Unit 6 and Unit 8. Meniscus cement is present in all kurkars, "rounding off" the remaining void where the primary pore space is still open.

According to infrared spectrophotometry, aragonite and low Mg-calcite are the major carbonate cement minerals. Quartz grains appear blue in cathodoluminescence micrographs, whereas fossils show a bright orange color. Superficial ooid rims around quartz nuclei sometimes appear in faint orange colors, whereas other cortex and pore-occluding micritic and sparitic cements are nonluminescent. Elemental distribution maps show no significant variations in the Mg, Na, Sr, Fe, and Mn content within the micritic and sparitic pore-occluding cements. Significant variations in the elemental content are only present in the cortex cements. Brownish microcrystalline rims, which are related to rhizolithes, show a higher Mg, Fe, and Na content than the surrounding micritic cements. Superficial ooids around quartz nuclei show enrichment in the Mg, Na, Sr, and Fe content.

To conclude, the kurkars at the "Atlit Railroad Bridge" section show distinct differences in textures and alteration processes which characterize the aeolianites.
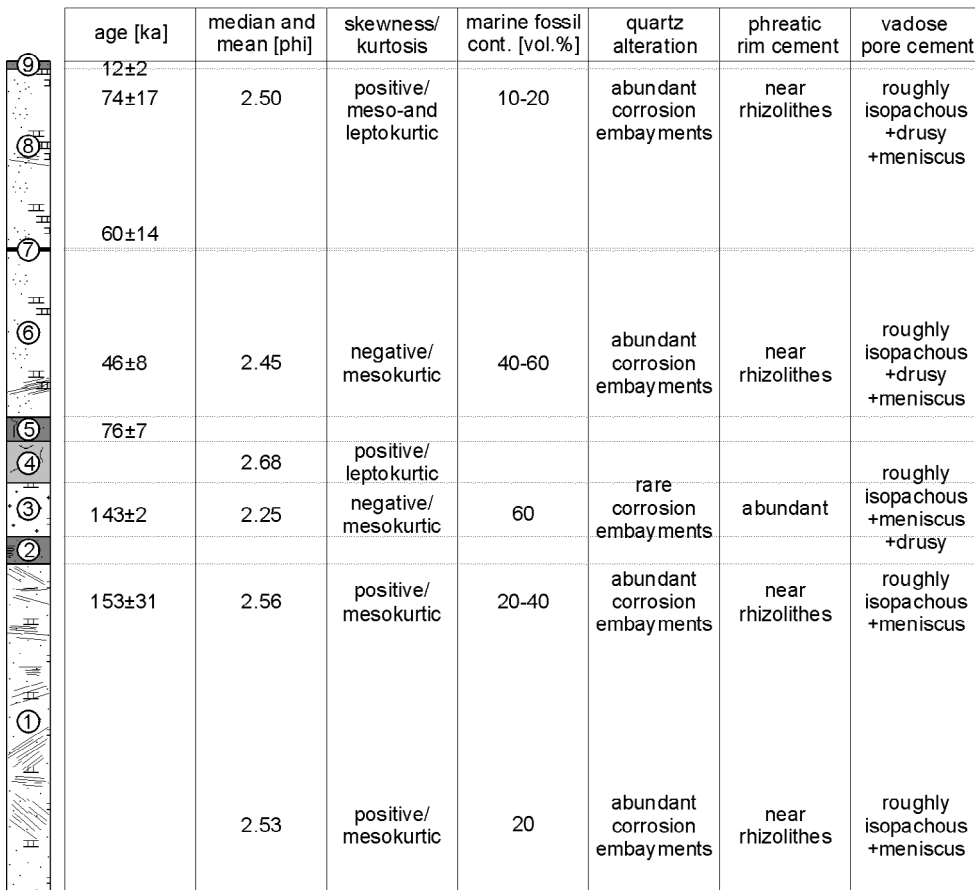
age [ka]	median and mean [phi]	skewness/ kurtosis	marine fossil cont. [vol.%]	quartz alteration	phreatic rim cement	vadose pore cement
12±2						
74±17	2.50	positive/ meso- and leptokurtic	10-20	abundant corrosion embayments	near rhizolithes	roughly isopachous +drusy +meniscus
60±14						
46±8	2.45	negative/ mesokurtic	40-60	abundant corrosion embayments	near rhizolithes	roughly isopachous +drusy +meniscus
76±7						
	2.68	positive/ leptokurtic		rare corrosion embayments	abundant	roughly isopachous +meniscus +drusy
143±2	2.25	negative/ mesokurtic	60			
153±31	2.56	positive/ mesokurtic	20-40	abundant corrosion embayments	near rhizolithes	roughly isopachous +meniscus
	2.53	positive/ mesokurtic	20	abundant corrosion embayments	near rhizolithes	roughly isopachous +meniscus

Fig. 4: Compiled profile of section "Atlit Railroad Bridge". No vertical scale. Luminescence age estimates from NEBER (2002) and FRECHEN et al. (in prep.). Facies attributes by particle size characteristics and petrographic textures. See Fig. 2 for legend.

4. Discussion

4.1. Chronostratigraphy and facies characteristics of aeolianites

The chronostratigraphic succession of the Quaternary ARB exposures (Fig. 4) is given in NEBER (2002), based on luminescence age estimates of FRECHEN et al. (in prep.). The sequence shows four major sand accumulation stages from ~160 ka onward, succeeded by episodes of marine transgression (~125 ka) or soil formation (~140, ~80, ~70, and ~10 ka). The documented aeolianites show distinct macro- and microscopic variations (Fig. 4) which can be attributed to particular depositional and early diagenetic environments, related to facies changes.

Initial aeolian sand deposition of a transverse ridge is documented by the Unit 1 aeolianite, with an depositional age of 153±31 ka (Fig. 4). The kurkar appears massive and large-scale cross bedding documents a barchanoid-like morphology. Dip directions of leeward sets indicate paleowind directions to the northwest (as today, see GOLDSMITH et al. 1990). The particle size distribution documents sorting processes during transport, due to aeolian forced migration over a considerable distance. Early diagenetic corrosion embayments of quartz grains result from silica replacement by invading carbonate (GAVISH & FRIEDMAN 1969, GOUDIE 1983). Silica dissolution and carbonate precipitation processes proceed at pore fluid pH conditions from 8.4 to 9.6 (KASHIK 1965, AMIEL 1975) which persist during subaerial chemical processes in semi-arid regions (GARDNER 1983).

Pore-occluding micritic to sparitic carbonates are documented by roughly isopachous rims, drusy mosaic and meniscus cements. All cements appear non luminescent and do not show significant variations in element concentration. MARSHALL (1988) and JAMES & CHOQUETTE (1990) have shown that nonluminescent, Fe-poor calcite cements precipitate under oxidizing conditions at high Eh, resulting from bacterial decay of organic matter. Hence, all pore-occluding cements of the aeolianites precipitated under these conditions, which are realized in the vadose meteoric environment. The open and uncompacted texture of the thin sections, as well as the nearly homogeneous element distribution, furthermore indicate a rapid precipitation during early diagenesis without significant changes in pore water chemistry.

The next major sand accumulation occurred around 143±27 ka and is documented by the aeolianite of Unit 3 (Fig. 4). This kurkar is characterized by abundant carbonate concretions and rhizolithes, which indicate that the sand was deposited under the restrictions of a vegetation cover, when plants trapped the encroaching sand and caused a vertical growth of the sequence. The particle size distribution does not show any sorting effects during transport and the sediment most likely accumulated close to the source, i.e. the shoreline. In addition, the poor sorting is characteristic of vegetated coastal dunes (McCANN & BYRNE 1989). Former pore space is occluded by vadose meteoric cements, like isopachous rims of roughly equant micrite, meniscus, and drusy mosaic calcite. Detrital particles, juxtaposed to rhizocretions, show brownish micritic cortex rims. None of the carbonate cements shows zonation in cathodoluminescence. In contrast, electron microprobe analysis reveal quantitative variations of Mg, Sr, and Fe, with higher contents in brownish rim cements in comparison to the pore-occluding vadose cements. According to JAMES & CHOQUETTE (1990), high Mg-calcite dissolution processes cause a release of magnesium and strontium in the percolating pore waters. Dissolution of present high Mg-calcite fossil shells and subsequent re-precipitation of carbonate cements occurred during the lithification of the aeolianites. Meteoric environment studies of McCLAIN et al. (1992) showed highest Mg and Sr values in the water column near the surface of fresh water lenses, where reducing conditions persist. Mg and Sr are incorporated in carbonate cements which precipitate in this environment. LAND (1970), AMIEL (1975), and GARDNER (1983) described high Mg, Sr, and Fe values in carbonate cements which originated from a reducing, phreatic meteoric milieu. Consequently - as the brownish cortex rim cements are more pronounced near rhizolithes, and show higher Mg, Sr, and Fe concentrations than the vadose pore-occluding cements - these brownish cements most likely precipitated in an at least temporarily phreatic environment of the water saturated plant root rhizosphere, possibly related to episodes of high precipitation.

Renewed sand accumulation between 46±8 and 74±17 ka (Fig. 4) lead to the elongated form of the exposed "kurkar ridge" and is represented by the aeolianites of Unit 6 and Unit 8. The distinct facies are separated by a carbonaceous hardpan, formed in a semi-arid environment. Macroscopic attributes are nodular carbonate, carbonate concretions, cemented rhizolithes and small patches of weakly cemented sand. The particle size distribution of the aeolianites indicates a short transport path of the sands and shows discrete differences between the kurkar units. Corrosion embayments of quartz grains are documented in thin sections as well as meteoric vadose and phreatic pore cements. Both aeolianites show abundant ooid cortex rims. These ooids show faint to bright orange cathodoluminescence colors and elemental distribution maps display higher Mg, Sr, Na, and Fe concentrations, in comparison to meteoric cements. These element concentrations, especially the presence of Fe, in the cortex cements indicate that carbonate precipitation was most likely related to reducing conditions, associated with a period of marine reworking of earlier deposited kurkar material before renewed aeolian transport and accumulation. In summary, the aeolianites at the "Atlit Railroad Bridge" section formed under semi-arid conditions with episodes of enhanced precipitation, documented by rhizolithes and related petrographic textures. Initial dune-sand accumulation of barchanoid like dunes is documented by the Unit 1 aeolianite, which dates back to the late OIS 6. The succeeding aeolianites accumulated when the dune system was already stabilized by a vegetation cover and the plants acted as a baffle and trapped the migrating aeolian sands. These multiple phases of sand encroachment, represented by the Unit 3, Unit 6, and Unit 8 kurkars, resulted in vertical growth of the sequence and the development of the morphological form of the coast parallel "kurkar ridge".

4.2. Paleoclimatic implications

Several sedimentary cycles of aeolian sand accumulation

and subsequent soil formation are documented in the Quaternary sequence of the ARB section dating from late OIS 6 to OIS 1. The established chronostratigraphical record of the sequence (Fig. 4), by luminescence age estimates given in Neber (2002) with methodological details in Frechen et al. (in prep.), allows an interpretation in terms of paleoclimate fluctuations. Semi-arid conditions with seasonal high precipitation episodes are suggested for stages of sand migration, accumulation and subsequent induration during early diagenesis of four aeolianites (Unit 1, Unit 3, Unit 6, and Unit 8). Surface stabilization is related to periods of reduced sand accumulation and dense vegetation growth, indicating distinct differences in humidity during and shortly after sand encroachment episodes. Prolonging intervals of surface stabilization and favorable environmental conditions led to periods of soil formation, documented as carbonaceous hardpan (Unit 7) or paleosols (Unit 2, Unit 5, and Unit 9). Soil formation occurred at around ~140, ~80, ~70, and ~10 ka.

The Unit 2 hamra horizon (~140 ka) reflects a humid period which clearly predates the marine transgression of OIS 5e, as soil formation took place before the deposition of the Unit 4 beachrock, which itself is associated with OIS 5e. Similar environmental conditions are postulated from climate archives in the Mediterranean region and northern Africa. Frumkin et al. (2000) postulated a period of high temperatures, enhanced precipitation, and a dense vegetation cover between 140 and 134 ka from speleothem studies in the eastern Israeli mountains. Isotope studies of Red Sea cores from Hemleben et al. (1996) showed a humid episode which peaked at 145 ka. Emeis et al. (2000) described an oxidized remnant ("ghost") of a sapropel formation period around 148 ka in cores from the eastern Mediterranean Sea. McKenzie (1993) as well as Wendorf et al. (1994) described lake level highstands from the eastern Sahara between 140 to 130 ka. Paleo-lake levels in Kenya have also been high during late OIS 6 with maximum elevations around 135 ka (Trauth et al. 2001).

Marine sediments related to OIS 5e are represented by a beachrock horizon. The marine highstand is also documented by beach boulder deposits along the Egyptian coast which have been dated with 121±6 ka by El-Asmar & Wood (2000). According to Hemleben et al. (1996), the continental climate during this period in the Red Sea area was characterized by humid conditions, with a maximum humidity peak at 122 ka. The transition from OIS 6 to OIS 5 in the eastern Sahara and the broader north African region is characterized by large freshwater lakes with high water levels until ~110 ka (McKenzie 1993, Wendorf et al. 1994). Anoxic conditions in the Mediterranean Sea and high Nile river discharge, triggered by a period of an intensive African monsoon, lead to the deposition of sapropel S5 at around 125 ka (Rossignol-Strick 1983, Cheddadi & Rossignol-Strick 1995, Lourens et al. 1996, Emeis et al. 2000).

The following hamra (Unit 5) is related to a humid period which centered at around 80 ka, whereas the subsequent carbonaceous hardpan (Unit 7) merely reflects a period of reduced sand accumulation, which enhanced soil formation at around ~70 ka. The pluvial stage is also documented in the cave records of the Israeli mountains, where it was dated in between 80 and 70 ka (Kaufman et al. 1998). Hemleben et al. (1996) detected a humid peak at around 80 ka in records

from the Red Sea. In addition, Wendorf et al. (1994) and Trauth et al. (2001) postulated a phase of increased precipitation prior to 70 ka in the eastern Sahara and in Kenya, respectively. Similar pluvial conditions are also documented in marine records by sapropel formation in the Mediterranean basin which occurred between 85 and 80 ka (Rossignol-Strick 1983, Cheddadi & Rossignol-Strick 1995, Emeis et al. 2000).

The uppermost hamra (Unit 9) in the "Atlit Railroad Bridge" sequence formed around ~10 ka. Cave records in Israel, studied by Frumkin et al. (2000), document that the period from 13 to 11 ka is characterized by enhanced precipitation and high temperatures. Magaritz (1986) and Goring-Morris & Goldberg (1990) postulated a humid episode and soil formation stage from 14 to 11 ka for the northern Negev desert. This period of enhanced precipitation is also documented in the Red Sea records from 13 ka onward (Almogi-Labin et al. 1991, Hemleben et al. 1996). Williams et al. (2000) reconstructed wet and warm climatic conditions for the phase from 11.5 to 11 ka from sediments at the White Nile Valley, Sudan. The marine record of the Mediterranean displays a humid episode with sapropel development with a temporal offset to the continental archives at 8 ka, according to Rossignol-Strick (1983), and Emeis et al. (2000).

In summary, all humid episodes with associated soil formation in the "Atlit Railroad Bridge" site are also reflected in other paleoclimate archives in the broader Mediterranean region and northern Africa.

5. Conclusions

The exposed "kurkar ridge" at the "Atlit Railroad Bridge" section displays four major sand accumulation stages either succeeded by soil formation periods (~140, ~80, ~70, and ~10 ka) or truncated by beachrock deposits (~125-120 ka). The documented aeolianites show distinct variations in macroscopic appearance, particle size distribution, and microscopic textures. These characterizing differences of the kurkars are related to facies differences. In general, all aeolianites are associated to semi-arid climate conditions during deposition and early diagenesis, with seasonal episodes of enhanced precipitation. Soil formation episodes are related to periods of enhanced precipitation.

The basal aeolianite of the section most likely resembles a transverse ridge with a barchanoid like morphology. Large-scale leeward cross beds indicate paleo-wind directions similar to the presently prevailing wind regime. This aeolianite was most likely deposited in considerable distance from the source, when beaches were more to the west during a stage of low sea level and sand migration was enhanced or even forced by a transgressing sea. Subsequent sedimentation of the shore near and already vegetated dune system is documented by an aeolianite, which is characterized by abundant rhizolithes. Encroaching sand was trapped by plants and resulted in vertical growth of the sequence. Renewed sand migration episodes lead to the elongated form of the "kurkar ridge". Hence, it seems conclusive that the coastal dune ridge formed from multiple stages of sand accumulation from late OIS 6 onward. Gvirtzman et al. (1998)

proposed that dune development occurred during a single event as longitudinal dunes during the Last Glacial, whereas TSOAR (2000) suggested a ridge development from foredunes. Both hypotheses have to be questioned. The complex sequence at the "Atlit Railroad Bridge" shows several periods of dune sand accretion and subsequent periods of dune stabilization from OIS 6 onward, with initial dune sand sedimentation of barchanoid like dunes.

The facies attributes of the sediments that form the "kurkar ridges" are related to climate fluctuations. The temporal succession of the exposed aeolianites and paleosols is in phase to continental and marine paleoclimate archives throughout the Mediterranean and northern Africa. The chronological record of the sedimentary sequences, associated facies and environment fluctuations, at the "Atlit Railroad Bridge" in the Carmel coastal plain document a sensitive and important paleoclimate archive from the late OIS 6 to OIS 1 in the Mediterranean region.

Acknowledgements

References

ADAMS, A.E. & MCKENZIE, W.S. (1998): A Colour Atlas of Carbonate Sediments and Rocks under the Microscope. - 180 p., (Manson Publishing Ltd.) London.

ALMOGI-LABIN, A., HEMLEBEN, C., MEISCHNER, D. & ERLENKEUSER, H. (1991): Paleoenvironmental events during the last 13,000 years in the Central Red Sea as recorded by Pteropoda. - Paleoceanography, 6: 83-98, Washington.

AMIEL, J.A. (1975): Progressive Pedogenesis of Eolianite Sandstone. - J. Sediment. Petrol., 45: 513-519, Tulsa.

AVNIMELECH, M. (1962): The main trends in the Pleistocene-Holocene history of the Israelian Coastal Plain. - Quaternaria, 6: 479-495, Rome.

BOENIGK, W., BRUNNACKER, K., RONEN, A. & TILLMANNS, W. (1985): Die Äolianite in der nördlichen Küstenzone von Israel; Genese, Stratigraphie und Klimageschichte. - Quartär, 35/36: 113-140, Bonn.

CHEDDADI, R. & ROSSIGNOL-STRICK, M. (1995): Improved preservation of organic matter and pollen in Eastern Mediterranean sapropels. - Paleoceanography, 10: 301-309, Washington.

EL-ASMAR, H.M. & WOOD, P. (2000): Quaternary shoreline development: northwestern coast of Egypt. - Quat. Sci. Rev., 19: 1137-1149, Oxford.

EMEIS, K.-C., SAKAMOTO, T., WEHAUSEN, R. & BRUMSACK, H.-J. (2000): The sapropel record of the eastern Mediterranean - results of Ocean Drilling Program Leg 160. - Palaeogeogr. Palaeoclimatol. Palaeoecol., 158: 371-395, Amsterdam.

EMERY, K.O. & NEEV, D. (1960): Mediterranean beaches of Israel. - Geol. Surv. Israel Bull., 26: 1-23, Jerusalem.

FARRAND, W.R. & RONEN, A., (1974): Observations on the Kurkar - Hamra Succession on the Carmel Coastal Plain, Israel. - Tel Aviv, 1: 45-54, Tel Aviv.

FOLK, R.L. & WARD, W.C. (1957): Brazos River bar: A study in the significance of grain-size parameters. - J. Sediment. Petrol, 27: 3-26, Tulsa.

FRECHEN, M., NEBER, A., ENGELMANN, A., TSATSKIN, A., BOENIGK, W. & RONEN, A. (in prep.): Chronological frame of the Pleistocene sedimentary cycles in the Carmel Coastal Plain of Israel.

FRIEDMAN, G.M. (1964). Early Diagenesis and Lithification in Carbonate Sediments. - J. Sediment. Petrol., 34: 777-813, Tulsa.

FRUMKIN, A., FORD, D.C. & SCHWARCZ, H.P. (2000): Paleoclimate and vegetation of the last glacial cycles in Jerusalem from a speleothem record. - Global Biogeochem. Cycles, 14: 863-870, Washington.

GARDNER, R.A.M. (1983): Aeolianite. - (In: GOUDIE, A.S. & PYE, K. (Eds.): Chemical sediments and geomorphology: Precipitates and Residua in the Near-Surface Environment), 265-300, (Academic Press) London.

GAVISH, E. & FRIEDMAN, G.M. (1969): Progressive Diagenesis in Quaternary to Late Tertiary Sediments: Sequence and Time Scale. - J. Sediment. Petrol., 39: 980-1006, Tulsa.

GOLDSMITH, V. & GOLIK, A. (1980): Sediment Transport Model of the Southeastern Mediterranean Coast. - Mar. Geol., 37: 147-175, Amsterdam.

GOLDSMITH, V., ROSEN, P. & GERTNER, Y. (1990): Eolian transport measurements, winds, and comparison with theoretical transport in Israeli coastal dunes. - (In: NORDSTROM, K., PSUTY, N. & CARTER, B. (Eds.): Coastal Dunes - Form and Process), 79-101, (John Wiley & Sons) Chichester.

GORING-MORRIS, A.N. & GOLDBERG, P. (1990): Late Quaternary dune incursions in the Southern Levant: Archaeology, Chronology and Palaeoenvironments. - Quat. Int., 5, 115-137, Oxford.

GOUDIE, A.S (1983): Calcrete. - (In: GOUDIE, A.S. & PYE, K. (Eds): Chemical sediments and Geomorphology: precipitation and residue in the near surface environment), 93-131, (Academic Press) London.

GVIRTZMAN, G., NETSER, M. & KATSAV, E. (1998): Last-Glacial to Holocene kurkar ridges, hamra soils, and dune fields in the coastal belt of central Israel. - Isr. J. Earth Sci., 47: 29-46, Jerusalem.

GVIRTZMAN, G., SHACHNAI, E., BAKLER, N. & ILANI, S. (1984): Stratigraphy of the Kurkar Group (Quaternary) of the Coastal Plain of Israel. - Geol. Surv. Israel, Current Res. 1983-84: 70-82, Jerusalem.

HEMLEBEN, C., MEISCHNER, D., ZAHN, R., ALMOGI-LABIN, A., ERLENKEUSER, H. & HILLER, B. (1996): Three hundred thousand year long stable isotope and faunal records from the Red Sea: Influence of global sea level change on hydrography. - Paleoceanography, 11: 147-156, Washington.

ISSAR, A. (1968): Geology of the Central Coastal Plain of Israel. - Isr. J. Earth Sci., 17: 16-29, Jerusalem.

ISSAR, A. (1980): Stratigraphy and Paleoclimates of the Pleistocene of Central and Northern Israel. - Palaeogeogr. Palaeoclimatol. Palaeoecol., 29: 261-280, Amsterdam.

ISSAR, A. & PICARD, L. (1971): On Pleistocene Shorelines in the Coastal Plain of Israel. - Quaternaria, 15: 267-272, Rome.

JAMES, N.P. & CHOQUETTE, P.W. (1990): Limestones - The Meteoric Diagenetic Environment. - (In: MELLREATH, J.A. & MORROW, D.W. (Eds.): Diagenesis), Geosci. Can. Repr. Ser., 4:35-73, Waterloo.

KARMELI, D., YAALON, D.H. & RAVINA, I. (1968): Dune Sand and Soil Strata in Quaternary Sedimentary Cycles of the Sharon Coastal Plain. - Isr. J. Earth Sci., 17: 45-53, Jerusalem.

KASHIK, S.A. (1965): Replacement of quartz by calcite in sedimentary rocks. Geochem. Int., 2: 133-138, Moscow.

KAUFMAN, A., WASSERBURG, G.J., PORCELLI, D., BAR-MATTHEWS, M., AYALON, A. & HALICZ, L. (1998): U-Th isotope systematics from the Soreq cave, Israel and climatic correlations. - Earth Planet. Sci. Lett., 156: 141-155, Amsterdam.

LAND, L.S. (1970): Phreatic versus vadose meteoric diagenesis of limestones: Evidence from a fossil water table. - Sedimentology, 14: 175-185, Oxford.

LOURENS, L.J., ANATONARAKOU, A., HILGEN, F.J., VAN HOOF, A.A.M., VERGNAUD-GRAZZINI, C. & ZACHARIASSE, W.J. (1996): Evaluation of the Plio-Pleistocene astronomical timescale. - Paleoceanography, 11: 391-413, Washington.

MAGARITZ, M. (1986): Environmental changes recorded in the Upper

Pleistocene along the desert boundary, Southern Israel. - Palaeogeogr. Palaeoclimatol. Palaeoecol., **53**: 213-229, Amsterdam.

MARSHALL, D.J. (1988): Cathodoluminescence of Geological Materials. - 1-146, (Unwin Hyman) Boston.

MCCANN, S.B. & BYRNE, M.-L. (1989): Stratification models for vegetated dunes in Atlantic Canada. - Proc. Royal Soc. Edinburgh, **96B**: 203-215, Edinburgh.

MCCLAIN, M.E., SWART, P.K. & VACHER, H.L. (1992): The Hydrogeochemistry of early meteoric diagenesis in a Holocene deposit of biogenic carbonates. - J. Sediment. Petrol., **62**: 1008-1022, Tulsa.

MCKENZIE, J.A. (1993): Pluvial conditions in the eastern Sahara following the penultimate deglaciation: implications for changes in atmospheric circulation patterns with global warming. - Palaeogeogr. Palaeoclimatol. Palaeoecol., **103**: 95-105, Amsterdam.

NEBER, A. (2002): Sedimentological properties of Quaternary Deposits on the Central coastal plain. - Unpublished Ph.D. dissertation, Department of Archaeology, University of Haifa, Israel.

NEEV, D., BAKLER, N. & EMERY, K.O. (1987): Mediterranean Coast of Israel and Sinai; Holocene tectonism from geology, geophysics and archeology. - 1-130, (Taylor and Francis) New York.

NEUSER, R.D. (1988): Zementstratigraphie und Kathodenlumineszenz des Korallenoolithen (Malm) im südniedersächsischen Bergland. - Bochumer Geologische und Geotechnische Arbeiten **32**: 1-17Bochum.

NEUSER, R.D. (1997): The present state of optical cathodoluminescence microscopy: developments and facilities at the Ruhr-University, Bochum. - Gaea heidelbergensis, **3**: 253, Heidelberg.

RONEN, A. (1975): The Palaeolithic Archaeology and Chronology of Israel. - (In: WENDORF, F. & MARKS, A.E. (Eds.): Problems in Prehistory: North Africa and the Levant), 229-248, (SMU Press) Dallas.

RONEN, A. (1977): Mousterian Sites in the red loam of Mount Carmel. - Eretz-Israel, **13**: 183-1190, Jerusalem.

RONEN, A., TSATSKIN, A. & LAUKHIN, S.A. (1999): The Genesis and Age of Mousterian Paleosols in the Carmel Coastal Plain, Israel. - (In: DAVIS, W.A. & CHARLES, R. (Eds.): Dorothy Garrod and the Progress of the Palaeolithic), 135-151, (Oxbow Books) Oxford.

ROSSIGNOL-STRICK, M. (1983): African monsoon, an immediate climate response to orbital insolation. - Nature, **304**: 46-49, London.

TRAUTH, M.H., DEINO, A. & STRECKER, M.R. (2001): Response of the East African climate to orbital forcing during the last interglacial (130-117 ka) and the early last glacial (117-60 ka). - Geology, **29**: 499-502, Boulder.

TSOAR, H. (2000): Geomorphology and paleogeography of sand dunes that have formed the kurkar ridges in the coastal plain of Israel. - Isr. J. Earth Sci., **49**: 189-196, Jerusalem.

WENDORF, F., SCHILD, R., Close, A.E., SCHWARCZ, H.P., MILLER, G.H., GRÜN, R., BLUSZCZ, A., Stokes, S., MORAWSKA, L., HUXTABLE, J., LUNDBERG, J., HILL, C.L. & MCKINNEY, C. (1994): A chronology for the Middle and Late Pleistocene wet episodes in the Eastern Sahara. - (In: BAR-YOSEF, O. & KRA, S (Eds.): Late Quaternary Chronology and Paleoclimates of the Eastern Mediterranean). 147-168, Radiocarbon, Tucson.

WILLIAMS, M.A.J., ADAMSON, D., COCK, B. & MCEVEDY, R. (2000): Late Quaternary environments in the White Nile region, Sudan. - Glob. Planet. Change, **26**: 305-316, Amsterdam.

YAALON, D.H. & DAN, J. (1967): Factors controlling soil formation and distribution in the Mediterranean Coastal Plain of Israel during Quaternary. - Proc. 7th INQUA Congr.: 321-338, Nevada.